Microbial Cell Factories

RESEARCH Open Access

Trichoderma virens XZ11-1 producing siderophores inhibits the infection of *Fusarium oxysporum* and promotes plant growth in banana plants

Haiyang Cui[1,2†], Qifeng Cheng[1,2†], Tao Jing[1,2], Yufeng Chen[1,2], Xiaojuan Li[1,2], Miaoyi Zhang[1,2], Dengfeng Qi[1,2], Junting Feng[1,2], Farinaz Vafadar[3], Yongzan Wei[1,2], Kai Li[1,2], Yankun Zhao[1,2], Dengbo Zhou[1,2*] and Jianghui Xie[1,2*]

Abstract

Background Banana Fusarium wilt caused by *Fusarium oxysporum* f. sp. *cubense* is a soil-borne fungal disease. Especially, tropical Race 4 (*Foc* TR4) can infect almost Cavendish subgroup and has a fatal threat to banana industry. Use of antagonistic microbes to manage soil-borne pathogen is viewed as a promising strategy.

Results Strain XZ11-1 isolated from tropical rainforest has the production ability of high siderophore. By the analysis of physiological and biochemical profiles, construction of phylogenetic tree, and comparative results from the NR database, strain XZ11-1 was identified as *Trichoderma virens*. A relative content of 79.45% siderophores was produced in the optimized fermentation solution, including hydroxamate and carboxylate-type siderophores. Siderophores were key for inhibiting the growth of *Foc* TR4 by competing for environmental iron. Similarly, *T. virens* XZ11-1 also had antagonistic activities against 10 phytopathogenic fungi. Pot experiments demonstrated that *T. virens* XZ11-1 could colonize in the root system of banana plants. The symbiotic interaction not only improve plant resistance to *Foc* TR4, but also enhance iron absorption of roots to promote plant growth by secreting siderophores.

Conclusions *T. virens* XZ11-1 with the high-yield siderophores was isolated and identified. The strain could effectively inhibit the infection of *Foc* TR4 in banana roots and promote plant growth. It is a promising biocontrol agent for controlling fungal disease.

Keywords *Trichoderma virens*, Siderophore, Banana Fusarium wilt disease, Biocontrol, Plant-growth promotion

†HaiYang Cui and Qifeng Cheng contributed equally to this work.

*Correspondence:
Dengbo Zhou
zhoudengbo@itbb.org.cn
Jianghui Xie
xiejianghui@itbb.org.cn

[1]School of Life and Health Sciences & College of Tropical Crops, Hainan University, Institute of Tropical Bioscience and Biotechnology, Chinese Academy of Tropical Agricultural Sciences, Haikou 571101, China
[2]National Key Laboratory of Biological Breeding of Tropical Crops, Chinese Academy of Tropical Agricultural Sciences, Sanya 572024, China
[3]Department of Agronomy and Plant Breeding, College of Agriculture, Isfahan University of Technology, Isfahan 84156-83111, Iran

Introduction

Banana (*Musa* spp.) is a key staple food and fruit in the developing countries. The banana industry plays a crucial role in improving global food security and increasing income [1]. Fusarium wilt disease caused by the soil-borne fungus *Fusarium oxysporum* f. sp. *cubense* (*Foc*) continue to threaten banana industry in global trade [2]. Specifically, *Foc* tropical race 4 (*Foc* TR4) is capable of infecting almost all banana cultivars, resulting in massive loss of banana yields [3]. While rotation can help reduce the disease incidence of *Foc* TR4 to some extent, farmers rarely employ this strategy due to its limited economic benefits [4]. To date, there has been a lack of immune varieties and effective chemical strategies for managing the disease [5]. In recent years, biocontrol strategies utilizing environmental microbes are as a promising approach for managing soil-borne fungal diseases [6]. These biocontrol agents (BCAs) are commonly used to control various agricultural pathogens. Among these, members of *Trichoderma spp.* belonging to the phylum *Ascomycota* are widely used as BCAs due to their antagonistic traits [7].

Previous studies showed that *Trichoderma* spp. can produce several bioactive secondary metabolites to inhibit the pathogenic growth [8]. Endophytic *Trichoderma* spp. in Korean ginseng and pine trees stimulate radishes growth via the release of bioactive metabolites [9]. Volatile organic compounds produced by *T. longibrachiatum* MK751759 inhibited the growth of *Sclerotium rolfsii* CSR [10]. Additionally, *Trichoderma* spp. also possess plant growth-promoting function [11–14]. *Trichoderma reesei* UH exhibited antagonistic activity against *Foc* and plant-growth promoting ability [15]. However, these strains are difficult to apply in the field due to diverse environment factors. The isolation and identification of high-efficient and widely-adapted *Trichoderma* is of great importance for controlling the spread of *Foc* TR4.

Iron is a vital trace element for the majority of organisms [16]. Despite the abundance of iron in the natural environment, the proportion of bioavailable iron is remarkably limited. This limitation is due to the rapid oxidation of iron by atmospheric oxygen, resulting in the formation of poorly soluble ferric oxyhydroxides [17]. Fe^{3+}-chelating molecules play a dual role in benefiting plants. First, they solubilize iron, making this typically unattainable nutrient accessible and thus promoting plant growth. Secondly, they inhibit the growth of pathogenic microorganisms by creating an environment starved of this indispensable micronutrient [18]. Siderophores, produced by plants, bacteria and fungi, are low-molecular weight chelating agents (200-2,000 Da). They exhibit a strong binding capacity for iron (III) [19]. For example, Sharma et al. reported that the siderophores produced by *Pseudomonas* strains GRP3A and PRS9 showed plant growth-promoting properties in maize [20]. Sulochana et al.demonstrated that the siderophore produced by *P. aeruginosa* JAS-25 promote the growth of pea plants [21]. Another research discovered that *Aureobasidium pullulans* strains L1 and L8 secrete siderophores to suppress the growth of *Monilinia laxa*, which prevent rot in peach fruits [22]. There are also related reports on siderophores produced by *Trichoderma* spp. Such as siderophores produced by *Trichoderma asperellum* Q1 has growth-promoting effects on *Arabidopsis thaliana* [23]. Manganiello et al. found that the siderophores Harzianic acid produced by *Trichoderma harzianum* can inhibit the growth of *Rhizoctonia solani* [24]. Numerous studies have documented the role of microbial siderophores in biocontrol and the enhancement of plant growth. However, studies focusing on *Trichoderma* siderophores with dual functions both in biocontrol and in promoting plant growth, particularly in banana cultivation are still need to be strengthened. Therefore, it is essential to isolate *Trichoderma* strains that produce siderophores and to explore their potential for biocontrol and enhancement of plant growth in banana cultivation.

In this study, we initially isolated strains capable of producing siderophores from a tropical rainforest. The selected strain XZ11-1 was identified using morphological, physiological, biochemical, and phylogenetic analysis. The siderophore production was optimized, followed by the identification of siderophore types. Furthermore, antifungal activities against *Foc* TR4 and other phytopathogenic fungi were assessed. The antifungal mechanism against *Foc* TR4 was analyzed through a cross-feeding experiment. Finally, a pot experiment was set for evaluating the biocontrol efficacy against banana Fusarium wilt and the plant-growth promoting of strain XZ11-1.

Materials and methods

Mushroom samples collection and fungal isolation

Mushroom (***Pluteus pantherinus Uchida***) samples were collected from the tropical rainforest of Qixianling, located in Baoting Li and Miao Autonomous County, Hainan, China (109°42'10.628" E, 18°42'28.713" N). The surfaces of mushrooms were washed and dried using sterilized water. Five grams of samples were ground to powder in liquid nitrogen and 45 mL of sterilized water were added. The suspension was shaken at 28 °C at 180 rpm for 30 min. The supernate was diluted from 10^-2 to 10^-3 and spread on the Bengal red culture media at 28 °C for 3 to 5 days [25]. Individual colony was transferred to PDA for purification. The purified strains were stored at -20 °C using 30% of glycerol preservation.

Measurement of siderophores in isolates

The Chrome Azurol S (CAS) assay was employed to screen for siderophore-producing strains [26]. The isolates were inoculated onto CAS detection solid plates and incubated at 28 °C for 3 to 5 days to observe the formation of orange transparent circles. The siderophores production was calculated by a liquid CAS assay [27]. Briefly, strains were inoculated into potato dextrose broth (PDB) medium at 28℃, 180 rpm for 3 days. After centrifugation at 8000 rpm for 3 min, 350 µL of cell-free supernatant (CFS) was added to reaction solution, including equal volume of CAS detection solution and 3.5 µL of shuttle solution. PDB medium was used as a control. Optical density at 630 nm of CFS (As) and controls (Ar) was measured at room temperature using a full-wavelength microplate reader (SynergyH1). The siderophore production was quantified using the following formula:

$$Siderophore\,Unit\ (P) = \frac{Ar - As}{Ar} \times 100\%$$

where As and Ar represented the absorbances of sample (CFS) and control at 630 nm, respectively.

Identification of strain XZ11-1

The siderophores-producing strain XZ11-1 was inoculated on PDA plates at 28 ℃ for 3 days. Morphological characteristics of mycelia and spores were observed by a scanning electron microscopy (SEM, Zeiss Sigma VP, Germany). The physiological and biochemical properties were determined, including the utilization of carbon and nitrogen sources and the tolerance to pH and sodium chloride [28]. Total DNA of strain XZ11-1 was extracted using the Rapid Fungal Genomic DNA Extraction Kit (Biotake, Beijing, China). The primer sequences of internal transcribed spacer (ITS) were ITS5 (GGAAGTAAA AGTCGTAACAAGG) and ITS4 (TCCGCTTATTGAT ATGC). The primers of the translation elongation factor 1α (TEF1α) were EF1 (ATGGGTAAGGARGACAAGAC) and EF2 (GGARGTACCAGTSATCATGTT). A total of 20 µL PCR system include 10 µL 2 × Taq Master Mix, 1 µL forward primer, 1 µL the reverse primer, 1 µL DNA template, and 7 µL ddH_2O. PCR reaction conditions: 94℃ pre-denaturation for 5 min, 94℃ denaturation for 30s, 55℃ annealing for 40s, 72℃ extensions for 1 min, 35 cycles, and 72℃ final extensions for 10 min. The PCR products were sequenced by using a Sanger-based automated sequencer (Sangon Biotech). The combination of two genetic loci, namely the TEF1 and ITS5 datasets were applied to construct the phylogenetic tree using the maximum likelihood method in MEGA Version 7.0 [25].

Genomic sequencing and functional annotation of strain XZ11-1

Libraries of genomic DNA were constructed using the Hieff NGS® MaxUp II DNA Library Preparation Kit for Illumina® (BioMarker). Their quantification was achieved with the Thermo Qubit 4.0 Fluorescence Quantification Instrument Q33226 (ThermoFisher). The sequencing was performed using the Illumina High-Throughput Sequencing Platform (HiSeq). FastQC was employed to assay the quality of raw sequencing data. PrInSeS-G was used for sequence correction to mitigate editing errors and the insertion or deletion of small fragments during splicing. GeneMark was used to predict genes, tRNAs, and rRNAs, etc. The repetitive sequences were identified using Repeat Masker [29]. Gene protein sequences were aligned with multiple databases, including CDD, KOG, COG, NR, NT, PFAM, Swissprot, and TrEMBL. The NR database alignment was used for species annotation and comprehensive analysis. The gene functions were annotated using Onotology (GO), euKaryotic Ortholog Groups (KOG) and Kyoto Encyclopedia of Genes and Genomes (KEGG) [28].

Effects of different Fe^{3+} concentrations on the growth of strain XZ11-1

The growth of strain XZ11-1 was analyzed on the iron-sufficient (addition of $FeCl_3$) and iron-deficient (addition of 2,2-dipyridyl) NA media (3.0 g of $NaNO_3$, 1.0 g of K_2HPO_4, 0.5 g of KCl, 0.5 g of $MgSO_4$, 30 g of sucrose, pH 7.0-7.2) [30]. $FeCl_3$ concentrations were set for 10 µM, 100 µM, and 300 µM. The 2,2'-bipyridine concentrations were set for 10 µM, 100 µM, 200 µM, and 300 µM). A blank medium was used as a control.

Evaluation of siderophores production capability of strain XZ11-1

Different concentrations of $FeCl_3$ (0 µM, 100 µM, 200 µM, 400 µM, 600 µM, 800 µM, 1000 µM, and 2000 µM) were added to the NA medium. The cultured strain XZ11-1 was inoculated into the NA medium at 28 °C and 180 rpm for 3 days. The siderophores production was detected using the CAS liquid detection method [27].

Detection of iron reducibility of strain XZ11-1 at different time points

One milliliter of fermentation broth of strain XZ11-1 was centrifuged at 8000 rpm for 2 min. 500 µL of supernatant was mixed with 25 µL of $FeCl_3$ (1.5 mM), 150 µL of sodium acetate buffer (5 M), and 75 µL of CAS (100 mM). 200 µL of the mixture was dropped into each well of a 96-well plate. Using an Enzyme Labeler, the absorbances of samples at 562 nm were measured within 3 min. The iron reduction activity was calculated using the following formula:

$$R = (A_{3min} - A_{0min}) / 3$$

where R was the iron reduction activity of sample, A_{0min} and A_{3min} represented the absorbance values of samples at the initial time point (Abs) and 3 min (Abs), respectively.

Identification of the siderophore types produced by strain XZ11-1

Strain XZ11-1 was cultured in PDB at 28 °C, 180 rpm for 3 days. Then, 1.5 mL of cultural liquid was transferred to 50 mL of iron-free NA medium and incubated under the same condition for 3 days. The fermentation broth was centrifuged at 12,000 rpm for 10 min to obtain a sterile cell-free supernatant (CFS) for further experiments. The spectrophotometric test was employed to detect carboxylate-type siderophores [31]. A mixture was prepared, including 0.5 mL of NA fermentation filtrate, 0.5 mL of 250 μM $CuSO_4$, and 1 mL of acetate buffer at pH 4.0. The formation of copper complex was observed in the spectral range of 190 to 280 nm to determine the maximum absorption. The absorption of copper complex does not occur at a particular wavelength. The entire wavelength ranging from 190 to 280 nm was scanned to identify the absorption peaks of siderophores using a UV-visible spectrophotometer (2802 UV/VIS Spectrophotometer, UNICO). Catecholate-type siderophores were detected using the Arnow's test [32]. 0.5 mL of fermentation supernatant was mixed with 0.5 mL of 0.5 M HCl and 0.5 mL of a reagent composed of 10 g of $NaNO_2$ and $Na_2MoO_4{\cdot}2H_2O$ each, dissolved in 100 mL of water. The solution color transferred from yellow to red by the addition of 1 M NaOH. The catecholic siderophores was confirmed by measuring the absorbance at 515 nm. Hydroxamate-type siderophores were detected using the $FeCl_3$ test [33]. 2% $FeCl_3$ of solution was dropped into 0.5 mL of fermentation supernatant. A hydroxamate siderophores was confirmed by observation of absorption peak within the range of 420–450 nm using a UV-visible spectrophotometer.

Broad-spectrum antifungal assay of strain XZ11-1

To test a broad-spectrum antifungal activities of strain XZ11-1, ten phytopathogenic fungi were selected as described by our previous reports [25], including *Fusarium oxysporum* f. sp. *cubense* tropical Race 4 (ATCC 76255), *Fusarium oxysporum* sp. *Lycopersici* (ATCC 16322), *Curvularia lunata* (ATCC 42011), *Colletotrichum fragariae* (ATCC 58718), *Colletotrichum gloeosporioides* (ATCC 16330) from banana, *Botrytis cinerea* (ATCC 208829), *Colletotrichum gloeosporioides* (ATCC 58222) from mango, *Fusarium graminearum* (ATCC 46779) from wheat plants with wheat head blight, *Pestalogiopsis sp.* (ATCC 26275) from plants with mango leaf blight, *Colletotrichum litchi* (ATCC 20438) from a decaying litchi. The identified phytopathogens were kept at Institute of Tropical Bioscience and Biotechnology, Chinese Academy of Tropical Agricultural Sciences. A conventional spot inoculation method was used to test the antifungal activity according to Long et al. [25]. A 5-mm mycelial disc of pathogenic fungi was placed on the edge of PDA plates. The same size disc of strain XZ11-1 was placed on the opposite side. The pathogenic mycelial disc alone was used as a control. All experiments were performed in triplicate.

Effect of strain XZ11-1 supernatant on the growth of *Foc* TR4

To confirm that strain XZ11-1 inhibits the growth of *Fusarium oxysporum* f. sp. *cubense* Tropical Race 4 (*Foc* TR4) through siderophore [34], three types of supernatants prodduced by strain XZ11-1 included: (1) supernatant obtained from iron-saturated conditions (strain XZ11-1 grown in iron-rich NA medium, where minimal siderophore production occurs, but other compounds are secreted; referred to as SNri), (2) supernatant obtained from iron-poor conditions (strain XZ11-1 cultured in iron-limited NA medium, sparking siderophore production plus other secreted compounds; denoted as SNli), and (3) supernatant from iron-poor conditions, which was then supplemented with 50 μM $FeCl_3$ (SNre). Although siderophores were present in this supernatant, they became ineffective for iron uptake due to the high iron concentration. Sterilized water was used as a control, replacing the supernatant (SNcontrol). Supernatant assays were performed in triplicate for all conditions. We inoculated 20 μL of *Foc* TR4 spore suspension (adjusted to 1 × 10^7 spores/mL, as determined by hemocytometer counting) into 1.8 mL of iron-limited NA medium (diluted 10-fold to better assess the effect of the supernatant) along with 200 μL of cell-free supernatant (CFS). The mixture were then incubated at 28 °C with shaking at 180 rpm. After 24 h, spore counts were determined using a hemocytometer, with triplicates for each treatment. Subsequently, we assessed the effect of strain XZ11-1 supernatant on pathogen development, comparing it with pathogen growth in supernatant-free conditions using the formula: $GE_{treatment} = ((SN_{treatment} \div SN_{control}) - 1) \times 100$, where $SN_{treatment}$ is SNli, SNri or SNre. For this computation, we consolidated the mean of supernatant impacts from the three experimental replicates. Recorded values less than zero were indicative of growth suppression, while those greater than zero were suggestive of growth promotion. The outcomes are articulated as the percentage variation in growth. From these measurements, we can determine the net Gravitational Equivalent (GE) of siderophores using the formula: GEnet = GEli - GEre.

Identification extracellular promotion ability of strain XZ11-1

Nitrogen-fixing ability

A diameter of 5 mm fresh mycelial disc was obtained and placed at the center of Ashby solid medium agar plate. The plates were inoculated in a constant temperature incubator at 28°C cultured for 5 days. If strain XZ11-1 can grow on Ashby solid medium, it indicates that it has nitrogen-fixing ability. Otherwise, it indicates the absence of nitrogen-fixing.

Phosphorus solubilization ability

A diameter of 5 mm fresh mycelial disc from strain XZ11-1 was placed at the center of inorganic phosphorus solid medium agar plate. The plates were inoculated at 28 °C cultured for 5 days. The ability of growing on inorganic phosphorus solid medium and generate phosphorus solubilization halos signifies its phosphorus solubilization capability. Conversely, the absence of growth indicates the lack of this ability.

Potassium solubilization ability

Following the method described above, the fresh mycelial disc of strain XZ11-1 were placed onto potassium solubilization solid medium agar plates. During the cultivation period, observe the growth of XZ11-1 on the plates and the formation of transparent zones.

IAA production ability

The Salkowski colorimetric method was used to measure IAA production ability. A 5 mm diameter agar plug was inoculated into King B liquid medium with 100 mg/L tryptophan. The medium was then incubated at 28℃, 180 rpm for 24 h. Subsequently, 350 µL of the fermentation broth was mixed with 700 µL of Salkowski's reagent (composed of 1 mL of 0.5 M $FeCl_3$ and 50 mL of 35% perchloric acid), wrapped in aluminum foil and left in the dark for 30 min. The depth of pink color development was indicative of the amount of IAA produced, with a deeper color higher the IAA production.

Colonization of strain XZ11-1 on banana roots

The roots of banana seedlings treated with strain XZ11-1 were observed using a scanning electron microscope (SEM, TM 4000 Plus, Hitachi, Tokyo, Japan). First, we conducted a hydroponic experiment, dividing the banana seedlings into two groups, one group was treated with sterile water, while the other group was treated with fermentation broth of strain XZ11-1 (Strain XZ11-1 was fermented in PDB at 28 °C, 180 rpm for 3 days, resulting in a spore concentration of 1×10^6). Three plants in each group. After 7 days of cultivation at room temperature, the banana roots were cut uniformly into pieces with 5 millimeters in length. Next, we soaked the samples in 2.5% (v/v) glutaraldehyde and fixed for 4 h, rinsed with PBS four times with 20 min for each time. Then, the samples were dehydrated using alcohol solutions of different concentrations (30%, 50%, 70%, 90%, and 100%). Subsequently, the samples were stored at -80 °C for 4 h. Finally, the dried samples were coated with a thin layer of gold and observed using SEM.

Assessment of plant growth promotion and biocontrol efficiency

A pot experiment was conducted to assess the effectiveness of strain XZ11-1 in controlling banana wilt disease and its growth-promoting effect on banana plants. The soil was collected from a banana plantation and sterilized in advance. Strain XZ11-1 was inoculated into 1 L of sterilized NA medium with 300 mL of iron-free solution. The culture was fermented at 28 °C, 180 rpm for 3 days. The fermentation broth was then filtered through four layers of sterile gauze and spores was adjusted to 1×10^6 CFU/mL using sterile water. *Foc* TR4 was inoculated in PDB at 28 °C, 180 rpm for 5 days. The culture was then filtered to obtain spore suspension of *Foc* TR4. The spore suspension was diluted to 1×10^6 CFU/mL. Healthy banana seedlings (*Musa* AAA group, Cavendish cv. Brazil) with uniform growth were selected and transplanted into pots (diameter 15 cm). After one week of cultivation in the greenhouse at a temperature of 28 °C ± 2 °C, the seedlings were divided into four groups. The experiment consisted of four treatments, including: Strain XZ11-1 fermentation broth (1×10^5 CFU/g soil) + *Foc* TR4 (1×10^5 CFU/g soil), *Foc* TR4 (1×10^5 CFU/g soil), iron-free NA Medium, and XZ11-1 fermentation broth (1×10^5 CFU/g soil). a mixture of 100 milliliters of each treatment was added to the roots of the banana seedlings every week. All treatments were conducted in triplicate with 5 pots in each repeat. At 45 days post-inoculation (dpi), the yellowing symptom of banana leaves and the disease indexes were recorded according to Zhang et al. [35]. Various physiological parameters of banana seedlings were assessed, such as chlorophyll content, stem diameter, plant height, leaf area, leaf thickness, dry weight, fresh weight, and leaf count, as outlined by Zhang et al. (2021) [36].

Hemolytic activity assay

Trichoderma virens XZ11-1 was cultured in the Columbia Blood Agar medium (CBA, Beijing Solarbio Biological Technology Co., Ltd.) at 28℃ for 3 days to evaluate its hemolytic activity. The generation of halo was positive for the hemolytic ability.

Statistical analysis

All experimental procedures were carried out using a completely randomized design. Each data point represents the mean ± standard deviation (SD) obtained from a

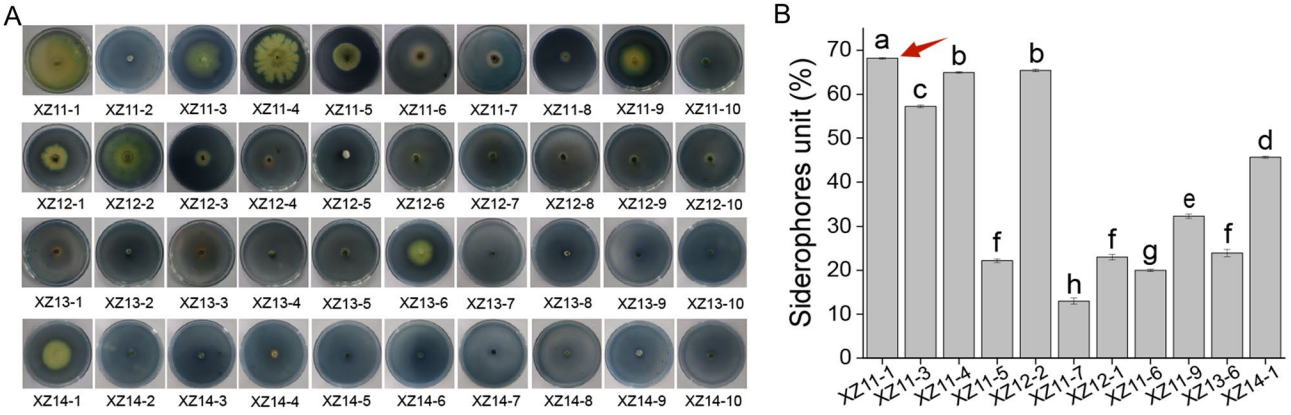

Fig. 1 Screening and identification of siderophores-producing strains. (**A**) CAS solid plate assay for the qualitative selection of siderophores-producing strains. (**B**) CAS liquid assay for the quantitative selection of siderophores-producing strains

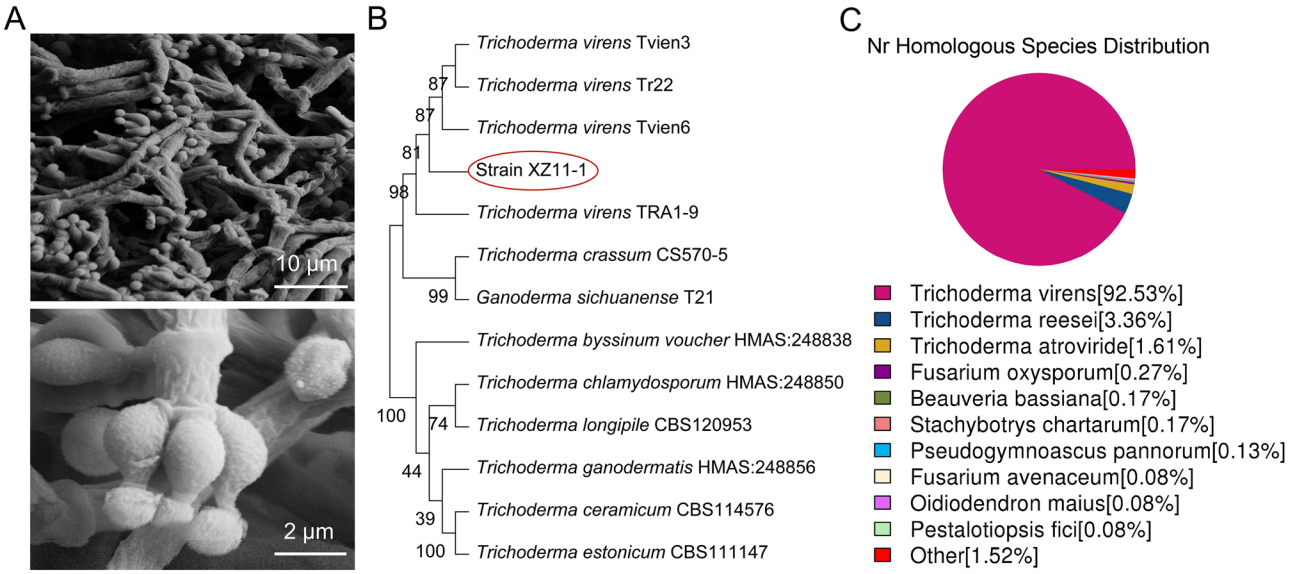

Fig. 2 (**A**) Scanning electron microscopy observation of the hyphal and spore morphology of strain XZ11-1. (**B**) Phylogenetic tree generated by maximum likelihood analysis based on the tandem sequence alignment of two genes (TEF1 and ITS4). (**C**) Species alignment results of the strain XZ11-1 genome in the Nr database

minimum of three biological replicates. Data analysis was performed using SPSS software, and the Duncan multiple range test was conducted at a statistical significance level set at $P < 0.05$.

Result

Isolation and screening of siderophores-producing strains

Forty fungi isolates were isolated from mushroom samples collected from the Qixianling Tropical Rainforest (Fig. S1A). Eleven strains can produce siderophores using the CAS plate assay (Fig. 1A). By calculation, strain XZ11-1 had the highest concentration of the siderophore with 68%. According to the function of siderophores in plant growth and antifungal properties, strain XZ11-1 was selected for the following experiment.

Identification of strain XZ11-1

Strain XZ11-1 demonstrates robust growth on PDA medium, producing abundant green aerial mycelia within 3 to 5 days (Fig. S1B). Scanning electron microscopy revealed that both the mycelium and aerial mycelium of strain XZ11-1 are branched. The conidia exhibited an ellipsoidal morphology aligned with the main axis, and the terminal conidia were characterized by thick cell walls and a globose to subglobose shape (Fig. 2A). Physiological and biochemical tests indicated that strain XZ11-1 effectively utilized all 19 carbon sources and 12 out of 19 nitrogen sources tested (Supplementary Table 1). It also demonstrated tolerance to pH levels ranging from 4 to 9 and NaCl concentrations of 1–3% (Supplementary Table 2). The PCR product was assembled using DNAMAN software, and after alignment with MAFFT

and editing with Gblocks, the TEF1 and ITS5 fragments were determined to be 1299 bp and 639 bp long, respectively. The evolutionary relationship of strain XZ11-1 was analyzed by constructing a phylogenetic tree using the TEF1 and ITS5 sequences, which showed that strain XZ11-1 clustered with *Trichoderma virens*, indicating a close evolutionary relationship between the two (Fig. 2B). Based on the genome comparison results from the Nr database (Fig. 2C), Strain XZ11-1 was identified as *Trichoderma virens*.

Genome assembly and annotation

The genome of strain XZ11-1 is comprised of 39,984,956 base pairs (bp), featuring a GC content of 48% and 2.06% repetitive sequences. A total of 11,904 genes have been predicted within the genome of strain XZ11-1, with an average sequence length of 1,743 bp (Fig. 3A; Supplementary Table 3). Out of these genes, 8,316 (69.86%), 5,903 (49.59%), and 3,326 (27.94%) were annotated using GO, KOG, and KEGG, respectively (Supplementary Table 4). The annotated genes were classified according to GO terms into three categories: cellular component, molecular function, and biological process (Fig. 3B). In the KOG classification, the pathways with the highest number of annotated genes included general function prediction, followed by posttranslational modification, protein turnover, chaperones, and the biosynthesis, transport, and catabolism of secondary metabolites (Fig. 3C). The metabolic pathways in KEGG were organized based on the relationship between KO and pathway, dividing them into five branches: genetic information processing, environmental information processing, metabolism, and cellular processes (Fig. 3D).

Growth status of strain XZ11-1 under varying iron concentrations

Strain XZ11-1 demonstrated significant growth advantages under conditions of abundant iron compared to

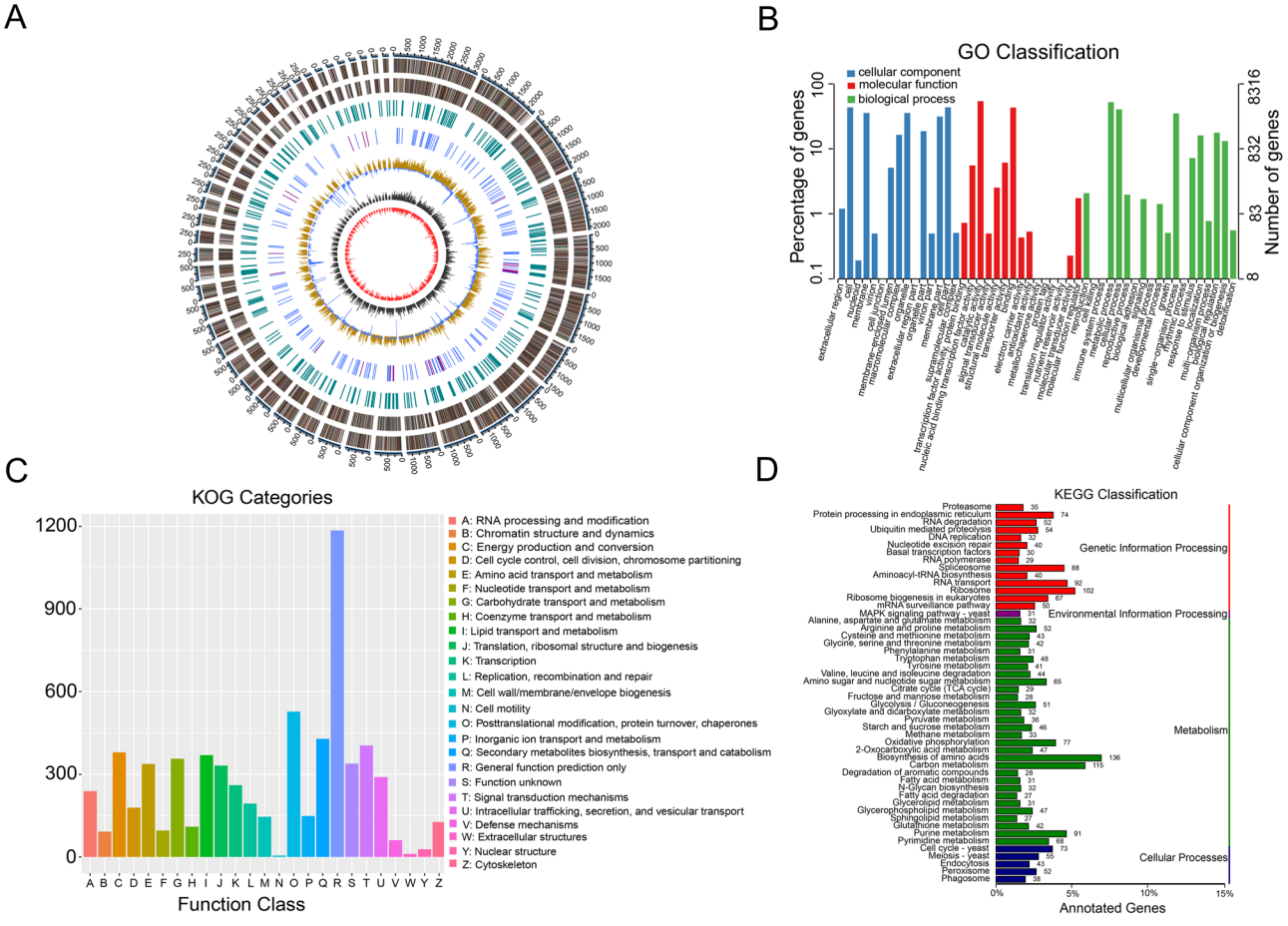

Fig. 3 Genomic information of strain XZ11-1 and functional annotation of predicted genes. (**A**) Gene circle map of strain XZ11-1. (**B**) Histogram of GO annotation. The horizontal axis was the secondary classification of GO and the vertical axis was the number of genes. Different colors represented different orthologs. (**C**) Histogram of KOG classification. Each color on the horizontal axis represented a functional classification of KOG and the vertical axis was the number of genes. (**D**) Classification of KEGG Pathway. The vertical axis was the name of the metabolic pathway and the vertical axis was the annotated of genes

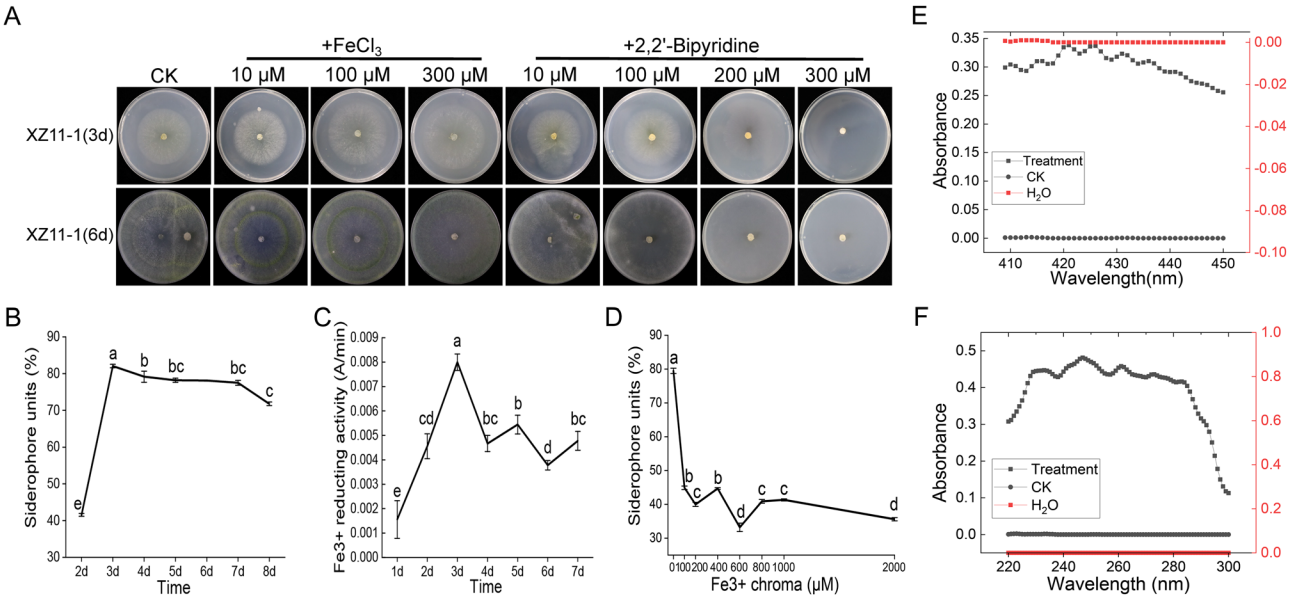

Fig. 4 The units and type of siderophores produced by strain XZ11-1. (**A**) The growth status of strain XZ11-1 on NA solid media plates supplemented with iron-rich (+$FeCl_3$) and iron-deficient (+2,2′-dipyridine) conditions, after continuous cultivation for 3 and 6 days. (**B**) Optimization of siderophores production of strain XZ11-1 under iron-limiting conditions across time gradient. (**C**) Detection of iron-reducing capability of strain XZ11-1 under iron-limiting conditions across a time gradient. (**D**) Variation in siderophores production of strain XZ11-1 after 3 days of fermentation culture under different Fe^{3+} concentrations. (**E**) Hydroxamate-type siderophore. Strain XZ11-1 absorption peaks were detected at 421 nm. (**F**) Carboxylate-type siderophores. Strain XZ11-1 absorption peaks were detected at 247 nm

the control (Fig. 4A). Mycelial growth increased with higher iron levels; however, it was noticeably reduced when the concentration of Fe^{3+} reached 100 μM. Furthermore, mycelial growth was inhibited when the availability of iron was restricted (> 10 μM with 2,2'-Bipyridine). At a concentration of 200 μM with 2,2'-Bipyridine, the absorption and utilization of iron were severely inhibited, leading to complete suppression of mycelial growth, with no observable signs of activity.

Optimization of siderophores production and detection of iron reduction ability of strain XZ11-1 under different conditions

The siderophore production and iron reduction capacity of strain XZ11-1 were assessed using a single-factor control variable approach. The findings indicated that on the 3rd day of fermentation, strain XZ11-1 exhibited the highest siderophore production and siderophore reduction capacity (Fig. 4B and C). A slight decrease in siderophore production was observed from the 4th to the 8th day (Fig. 4B). Additionally, on the third day of fermentation, the siderophore production of strain XZ11-1 was evaluated at various Fe^{3+} concentrations. The results revealed that under iron-limiting conditions, the highest siderophore production was 79.45%, while at 600 μM of Fe^{3+}, the lowest siderophore production was 33.21% (Fig. 4D).

Identification of siderophore types produced by strain XZ11-1

After 3 days of fermentation, the supernatant was collected. A 2% $FeCl_3$ solution was added to 0.5 mL of the supernatant using the $FeCl_3$ method, resulting in a color change to red. Subsequently, a full-wavelength scan revealed an absorption peak at 421 nm, indicating the presence of hydroxamate siderophores in the supernatant (Fig. S1C, Fig. 4E). Carboxylate-type siderophores were identified through Shenker's test, with an absorption peak at 247 nm detected in the supernatant (Fig. 4F). In the Arnow's test, no color change was observed in the solution, and no absorption peak was detected at 515 nm. Therefore, it can be concluded that the strain XZ11-1 produces both hydroxamate and carboxylate-type siderophores.

Strain XZ11-1 exhibiting the broad-spectrum antifungal activity

Ten phytopathogenic fungi were selected to assess the broad-spectrum antagonistic potential of strain XZ11-1. The findings revealed that strain XZ11-1 displayed significant antifungal ability against the tested fungi, with inhibition rates ranging from 50.91 to 65.52% (Fig. 5A). Particularly noteworthy is the strong inhibitory activity of *Trichoderma virens* XZ11-1 on the mycelial growth of *C. gloeosporioides* (ATCC 16330), *C. lunata* (ATCC 42011), *C. litchi* Trag (ATCC 20438), and *F. oxysporum* Race 4 (ATCC 76255), with inhibition rates of 65.52%, 65.52%,

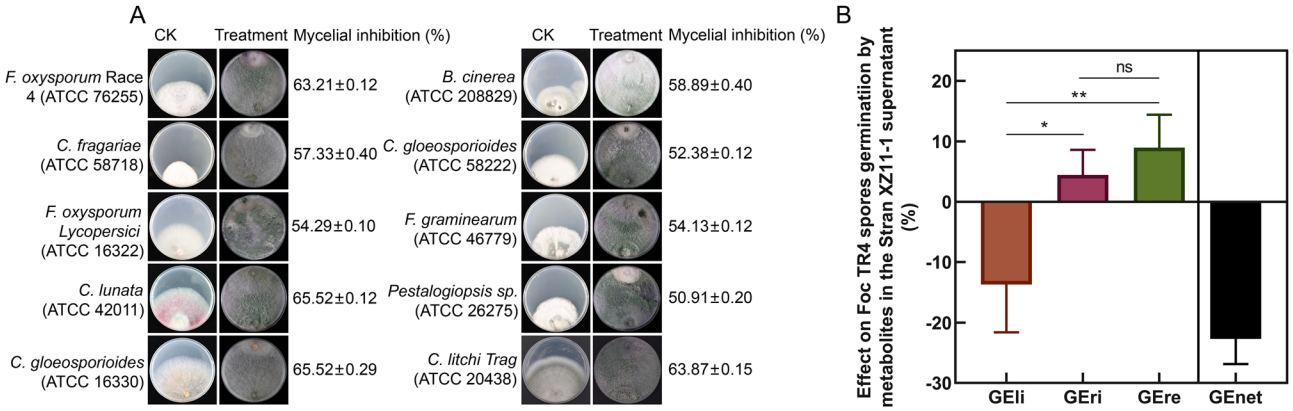

Fig. 5 Broad-spectrum inhibitory efficiency test of strain XZ11-1 against 10 phytopathogenic fungi and the impact of its metabolites production on the growth of *Foc* TR4. (**A**) Broad-spectrum inhibition efficiency test of strain XZ11-1 against 10 phytopathogenic fungi. (Data are expressed as mean ± standard deviation). (**B**) GEli: The growth effects were measured in supernatant collected under iron-limited (high siderophore concentration + other secreted metabolites), GEri: iron-rich (low siderophore concentration + other secreted metabolites), and GEre: iron-limited conditions replenished with iron (siderophore effect removed, while the effect of other metabolites is retained). GEnet: The net effect caused by siderophores alone (right column) was obtained by subtracting the growth effect of the iron-replenished supernatant from the growth effect of the iron-limited supernatant. The values indicate the percentage fold-change in growth

63.87%, and 63.21%, respectively. These results indicate that *Trichoderma virens* XZ11-1 possesses extensive antifungal properties.

The effect of *Trichoderma virens* XZ11-1 on the growth of *Foc* TR 4 mediated by siderophores

We evaluated the metabolites produced by strain XZ11-1 to determine their effects on the growth of *Foc* TR4. Our results indicated that the supernatant collected under iron-rich conditions, which contained a low concentration of siderophores, slightly enhanced the growth of *Foc* TR4. In contrast, treatment with the supernatant obtained under iron-limiting conditions, characterized by a high concentration of siderophores, significantly inhibited the growth of *Foc* TR4. When the pathogen was exposed to iron-starved supernatant supplemented with iron to reduce iron competition, the addition of iron neutralized the effects of the siderophores while preserving the influence of other secreted metabolites on pathogen proliferation (Fig. 5B). Our findings suggested that the iron-starved supernatant, when supplemented with iron, exhibited similarly weak promoting effects as the iron-rich supernatant, indicating that siderophores are the primary factor driving the inhibition of *Foc* TR4 growth under iron-limiting conditions.

The direct growth-promoting properties of strain XZ11-1

The abilities of nitrogen fixation, phosphorus solubilization, potassium solubilization, and indole-3-acetic acid (IAA) production were assessed using specific culture media. The results indicated that strain XZ11-1 was capable of growing on nitrogen-fixing and phosphate-enriched media. However, it did not produce a clear zone of phosphate solubilization, suggesting a lack of phosphate solubilization capability. Furthermore, strain XZ11-1 did not thrive in potassium-solubilizing media, indicating an inability to solubilize potassium (Fig. S2A). The colorimetric reaction between bacterial strain XZ11-1 and Salkowski's reagent for IAA production did not show any significant color change compared to the control group (CK), indicating that this strain does not possess the ability to produce IAA (Fig. S2B).

Colonization of strain XZ11-1 on banana roots

Under the scanning electron microscope at 400x magnification, the surface of banana roots in the control group appeared smooth with no attached mycelia (Fig. 6A). In contrast, banana roots treated with XZ11-1 displayed a significant amount of mycelia attached to the surface, interweaving in a complex pattern (Fig. 6B). These findings suggest that strain XZ11-1 can effectively colonize banana roots. Results of the hemolysis experiments are shown, the absence of a hemolytic zone surrounding strain XZ11-1 indicated that this strain was nonpathogenic to blood cells (Fig. S3).

Banana growth promotion and biocontrol effect of strain XZ11-1 in pot experiment

In vitro conditions, strain XZ11-1 demonstrated an inhibitory effect against various phytopathogenic fungi through siderophores mediation. This provides a basis to evaluate its biocontrol efficiency against *Foc* TR 4 and promote the growth of banana plants through pot experiments. In the biocontrol pot experiment, disease symptoms were observed on banana seedlings after 45 days of inoculation (dpi) in the control group, where banana seedlings exhibited symptoms of chlorosis at the leaf base (Fig. 7A). In contrast, the treatment with strain XZ11-1

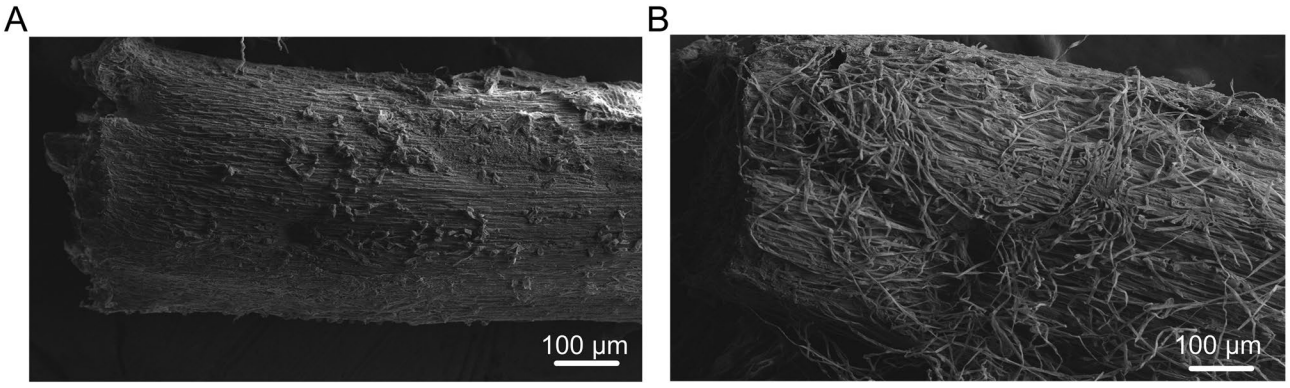

Fig. 6 Colonization of strain XZ11-1 in banana roots. (**A**) SEM observations after sterile water treatment. (**B**) SEM observations of banana roots after treatment with strain XZ11-1

displayed no evident disease symptoms on the leaves. Additionally, the corms exhibited black symptoms due to *Foc* TR4 infection, while no obvious black symptoms were observed in the strain XZ11-1 treatment. Comparing with the control group, the disease index decreased from 68.33 ± 1.17 to 26.67 ± 0.92 after the strain XZ11-1 treatment. The biocontrol efficiency was 60.98% (Fig. 7B). The growth of banana plants was inhibited because of *Foc* TR4 infection (Fig. 7C–I). The treatment group showed significant differences in chlorophyll content, stem diameter, plant height, leaf area, leaf thickness, dry weight, and fresh weight, with increases of 83%, 48%, 34%, 83%, 25%, 60%, and 83%, respectively. In the growth-promoting pot experiment, it was found that *Trichoderma virens* XZ11-1 significantly promoted banana growth compared to the control treatment (Fig. 8A). Compared to the control, the treatment exhibited significant differences in chlorophyll content, stem diameter, plant height, leaf area, leaf thickness, dry weight, and fresh weight, with increases of 76%, 46%, 31%, 91%, 72%, 54%, and 67%, respectively (Fig. 8B–I). Therefore, strain XZ11-1 not only plays a positive role in the control of *Foc* TR4, but also has a significant effect on promoting the growth of banana seedlings.

Discussion

Banana Fusarium wilt (BFW), caused by *Foc* TR4, is a serious disease that devastates the global banana industry. Once a banana plantation is infected, it will no longer be able to continue planting bananas. Currently, there is no effective chemical agent to control the disease. In China, comprehensive management strategies focusing on biological control techniques have demonstrated remarkable efficacy. Beneficial microorganisms from the natural environment are crucial in the biocontrol of banana Fusarium wilt. Therefore, selecting the appropriate natural environment is key to obtaining excellent BCAs. The tropical rainforest of China is characterized by high jungle perennial vegetation and environmental conditions with high temperatures and annual rainfall. These characteristics make these environments optimal for fostering a high diversity of fungi [37]. Especially, the abundant mushrooms in tropical rainforests are particularly important as isolation media for *Trichoderma* spp. [38]. In our study, forty fungi isolates were isolated from the mushroon samples indicated the abundant fungi species in tropical rainforests. we identified the *Trichoderma virens* XZ11-1, while traditional methods commonly rely on comparing ITS sequences for fungal species identification, this approach may have difficulty distinguishing closely related species. To enhance the accuracy of species identification, multiple gene sequences can be concatenated, thereby increasing the number of informative loci [25] *Trichoderma spp.* has been extensively utilized to combat fungal diseases. Swain et al. isolated strains of *Trichoderma* from tree bark that effectively controlled three types of soil-borne pathogenic fungi [39]. Rajani et al. isolated endophytic *Trichoderma* strains that significantly inhibited three plant pathogenic fungi through their volatile organic compounds (VOCs) [10].

The registration of over 200 *Trichoderma* species as potential biocontrol agents and plant growth promoters has led to mang studies aimed at understanding their mechanisms of action, particularly mycoparasitism and competition [40]. Currently, research on the antifungal mechanisms of *Trichoderma virens* mainly focuses on hyperparasitism and antibiosis. Guzmán-Guzmán et al. showed that *T. virens* produce trichodermamides, and various compounds including azaphilones, viridins, nitrogen heterocyclic compounds (e.g., harzianopyridone and harzianic acid), and volatile terpenes. *T. virens* use these compounds as a strong mechanism of action against several plant pathogens including *R. solani*, *C. heterostrophus*, *S. rolfsii* and *B. cinerea* [7]. Savani et al. reported that *T. reesei* has the potential to stimulate plant growth and control BFW through the production of indole acetic acid, siderophore, and hydrogen cyanide [15]. However, there are limited reports on the efficacy of *T. virens* against *Foc* TR4. In particular, research on

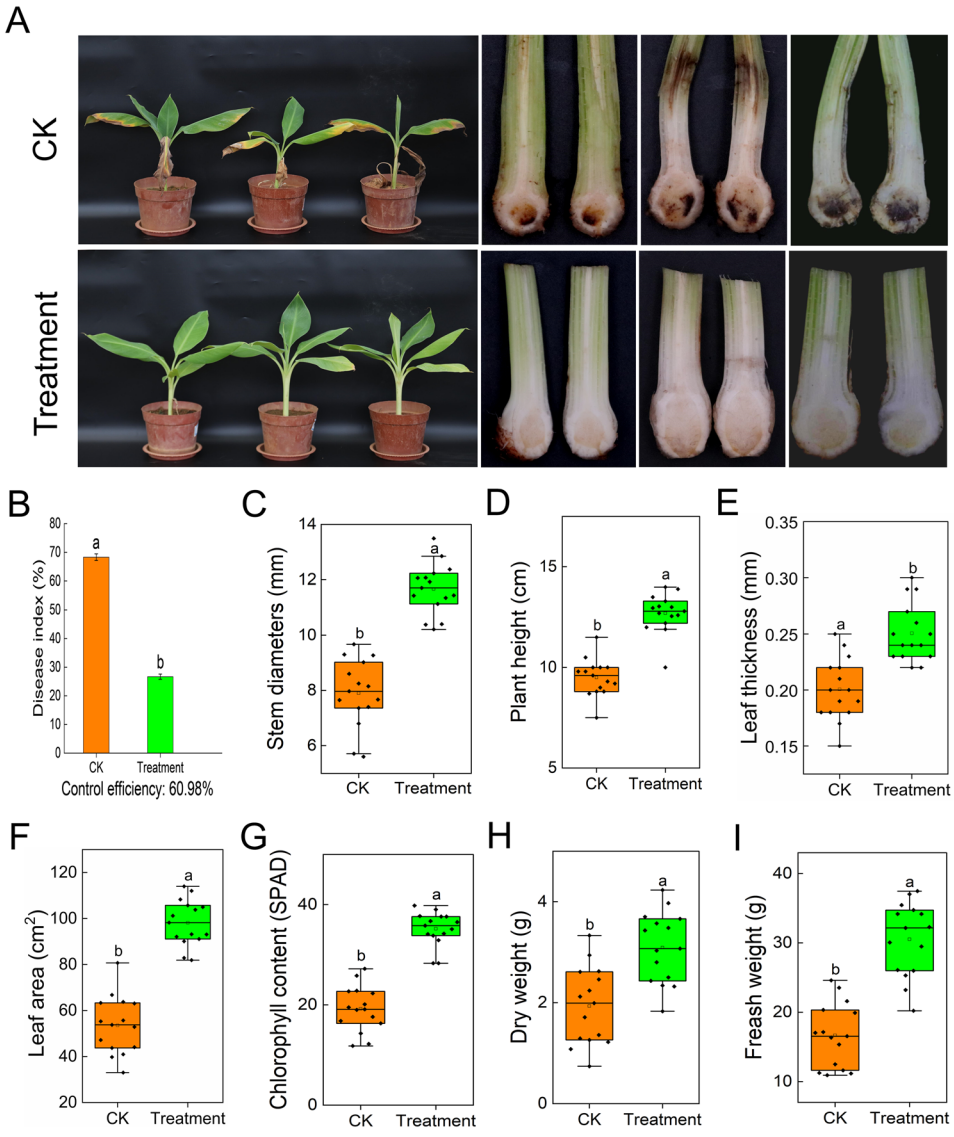

Fig. 7 Evaluating the biocontrol effect of strain XZ11-1. (**A**) Growth status of control (*Foc* TR4) and treatment (strain XZ11-1 + *Foc* TR4) at 45 dpi. The blackened part of the tuber is the infection site of *Foc* TR4. (**B**) Statistical analysis of disease indices. (**C**) Stem diameters (mm). (**D**) Plant height (cm). (**E**) Leaf thickness (mm). (**F**) Leaf area (cm^2). (**G**) Chlorophyll content (SPAD). (**H**) Dry weight (**I**) Fresh weight (g). Different lowercase letters indicate significant differences at the level of $p < 0.05$

the siderophores-producing strains of *T. virens* remains unexplored. In order to further understand the siderophores produced by *T. virens* XZ11-1, we optimized the conditions of siderophores production and identified the types of siderophores. Chowdappa et al. isolated a collection of fungi with the ability to produce hydroxamate siderophores. Notabley, *Penicillium chrysogenum* (CAL1) exhibited the highest siderophores yield at 57%, increasing to 73% after optimization. In comparison, Under iron-limiting conditions *T. virens* XZ11-1 exhibited the highest siderophores yield at 79.45%. So, *T. virens* XZ11-1 is characterized as a high-yielding siderophore-producing fungus [41]. In a high-iron environment of 600 μM $FeCl_3$, the siderophores yield of strain XZ11-1 was 33.21%. This indicates that iron-deficient conditions stimulate *T. virens* XZ11-1 to secrete siderophores to obtain the required iron, and the result is consistent with previous reports [42]. Upon further identification, we discovered that *T. virens* XZ11-1 produces hydroxamate-type and carboxylate-type siderophores. Mark et al. demonstrated that *Absidia corymbifera* and eight other fungal species can produce hydroxamate-type siderophores [43]. Interestingly, the hydroxamate-type siderophores uptake system delivers an antibiotic directly into targeted pathogens [44]. Furthermore, the hydroxycarboxylate-type siderophore, Xanthoferrin, as an important virulence factor of *X. campestris* pv. *campestris* which promotes plant growth through the sequestration of Fe^{3+} [45]. Gu et al.

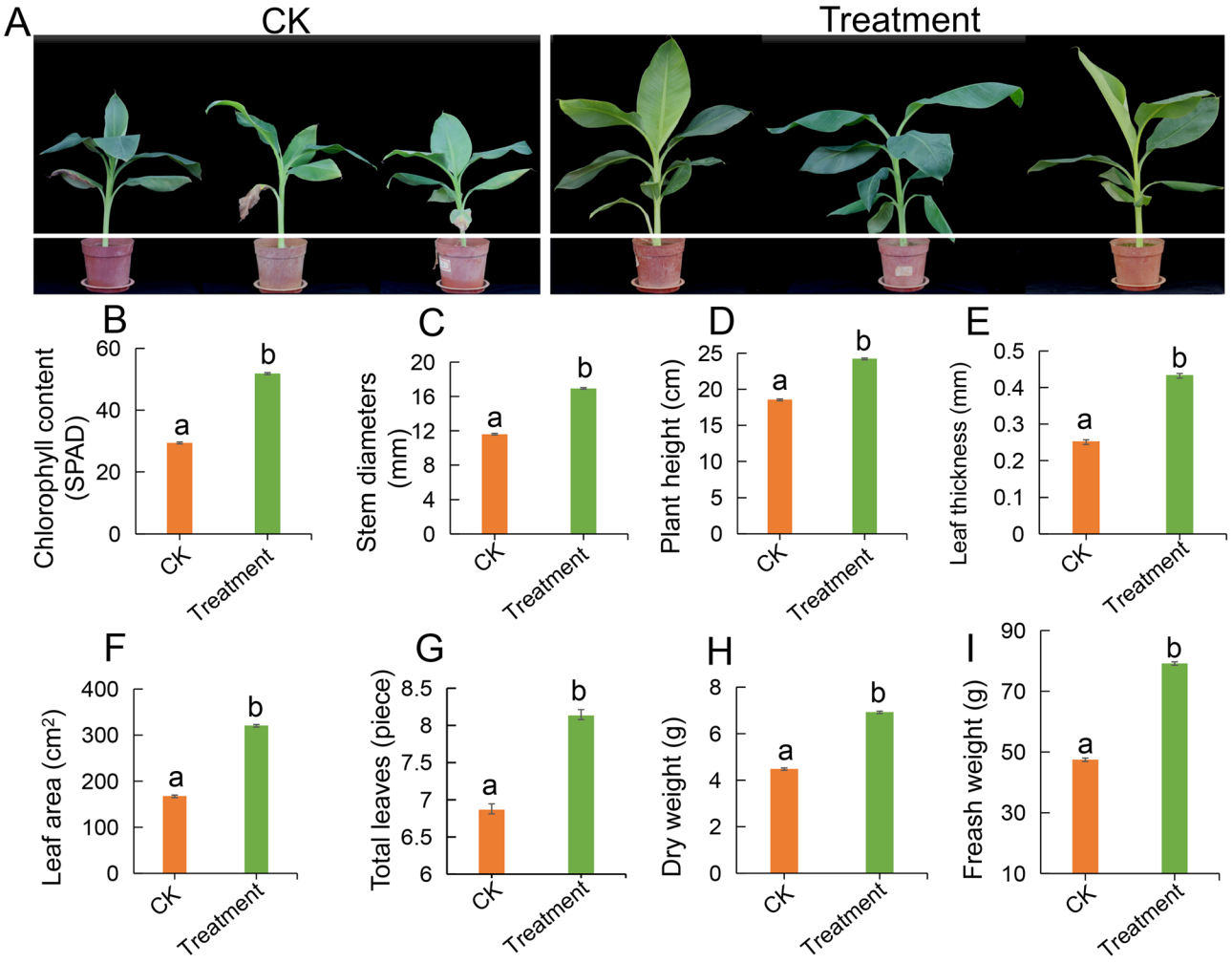

Fig. 8 Evaluation of the effect of strain XZ11-1 on banana plant growth promotion. (**A**) Growth status of control (NA) and treatment (strain XZ11-1) at 45 days. (**B**) Chlorophyll content (SPAD). (**C**) Stem diameters (mm). (**D**) Plant height (cm). (**E**) Leaf thickness (mm). (**F**) Leaf area (cm^2). (**G**) Total leaves (piece) (**H**) Dry weight (g) (**I**) Fresh weight (g). Different lowercase letters indicate significant differences at the level of $p < 0.05$

have verified the primary driver of antagonism against tomato bacterial wilt is siderophores through cross-feeding methods. Our study also used cross-feeding methods to confirm *T. virens* XZ11-1 inhibits *Foc* TR4 through siderophores [34]. The results indicated that iron-replenished supernatant exhibited similar mildly promotive effects as iron-rich supernatant. However, the growth of *Foc* TR4 was significantly inhibited after treatment with the iron-limited supernatant. These findings align with the results presented by Gu et al. [34]. This indicated that under iron-limiting conditions, siderophores are the primary driving factor in inhibiting the growth of *Foc* TR4. In pot experiment, When treated with *T. virens* XZ11-1, the biocontrol efficiency reached 60.98%. Similarly, endophytes *T. reesei* UH exhibited a resistance against BFW by delaying the onset of foliar symptoms to decrease disease severity [15]. These findings suggest that *T. virens* XZ11-1 has a potential as a valuable biocontrol resource.

Growth promoter is another important function for *Trichoderma spp.* López et al.identified *Trichoderma* species from Misiones Province in Argentina, including *T. atroviride* LBM 112, *T. stilbohypoxyli* LBM 120, and *T. koningiopsis* LBM 219, which significantly increased the dry weight of yerba mate seedlings by more than 47% and the aerial part by 24%. *T. koningiopsis* LBM 219 increased 25% of root dry weight compared to the control [46]. The symbiotic relationship between *Trichoderma* and roots not only improves plant growth, but also enhances the plant's immune response against pathogens [47, 48]. The *Trichoderma* resides among living plant cells, an interaction reminiscent of the initial stages of assault by soil-borne pathogens [49]. This symbiosis is facilitated partly through the release of volatile organic compounds (VOCs) and secretory factors, while the other mechanism relies on the colonization of fungal mycelia. For instance, the *Trichoderma* strain Tv-1511 exemplifies this phenomenon by enhancing the growth and

photosynthetic efficiency of mint roots upon colonization, leading to increased production of mint essential oil [50]. Based on these studies, our research aimed to verify the colonization ability of *T. virens* XZ11-1 in banana roots. Due to the difficulty of directly observing this interaction in the soil, we chose to adopt a hydroponic experimental approach. Using scanning electron microscopy, we observed strain XZ11-1 hyphae and penetration tubes adhering to banana roots, which aligns with the observations of Garstecka Z and Antoszewski M, who also utilized hydroponics to observe *Trichoderma* hyphae entwined around plant roots [51]. In the pot experiment, the treated banana seedlings exhibited superior growth advantages in terms of chlorophyll content, plant height, leaf area, leaf thickness, number of leaves, dry weight, fresh weight, and stem thickness compared to the control. However, strain XZ11-1 lacks the ability for phosphorus solubilization, potassium solubilization, and indole-3-acetic acid (IAA) production. Despite this, it has the capability to establish stable colonization in the root region of bananas. It is hypothesized that *T. virens* XZ11-1 promotes banana growth through the secretion of siderophores, which sequester unavailable environmental Fe^{3+} for bananas, providing crucial iron nutrients. Further research is needed to confirm whether the promotion of banana growth is directly facilitated by siderophores. Therefore, *T. rivens* XZ11-1 not only acts as an antagonist against *Foc* TR4 but also enhances banana growth by secreting hydroxamate and carboxylate types of siderophores. In the subsequent experiments, we will continue to carry out pot experiments under different pathogen inoculation conditions to expand the application range of this biocontrol agent.

Conclusion

This study uncovered the role of *Trichoderma virens* XZ11-1 in biocontrol and growth promotion. Nevertheless, further research need to discuss the interaction mechanism between *Trichoderma virens* XZ11-1 and plant roots. We will further analyze the synergistic effects of its application on the microbial community structure. The study will be benefit for the utilization of functional microorganisms in sustainable agricultural development.

Supplementary Information

The online version contains supplementary material available at https://doi.org/10.1186/s12934-024-02626-4.

Supplementary Material 1

Author contributions

HYC and QFC carried out the experiments and drafted the manuscript. TJ and YFC Data curation and reviewed the manuscript. XJL, MYZ and DFQ analyzed the data and draw the Fig. 1, 2, 3. FV edited the manuscript. YZW designed the experiments. KL and YKZ designed the pot experiment. DBZ and JHX responsible for supervising the overall work and writing the final manuscript. All authors read and approved the final manuscript.

Funding

This work was supported by the Natural Science Foundation of Hainan (321RC1094, 322QN417), Chinese Academy of Tropical Agricultural Sciences for Science and Technology Innovation Team of National Tropical Agricultural Science Center (NO. CATASCXTD202312), Central Public-interest Scientific Institution Basal Research Fund (NO.1630092022002), the National Natural Science Foundation of China (32360706), the China Agriculture Research System (CARS-31), the Project of National Key Laboratory for Tropical Crop Breeding (No. NKLTCB202311).

Data availability

No datasets were generated or analysed during the current study.

Declarations

Competing interests

The authors declare no competing interests.

Received: 29 April 2024 / Accepted: 17 December 2024
Published online: 16 January 2025

References

1. Xie L, Wu Y, Duan X, Li T, Jiang Y. Proteomic and physiological analysis provides an elucidation of Fusarium proliferatum infection causing crown rot on banana fruit. Microbiol Res. 2022;256:126952.
2. Zou N, Zhou D, Chen Y, Lin P, Chen Y, Wang W, Xie J, Wang M. A novel antifungal actinomycete *Streptomyces* sp. strain H3-2 effectively controls banana Fusarium wilt. Front Microbiol. 2021;12:706647.
3. Yun T, Zhang M, Zhou D, Jing T, Zang X, Qi D, Chen Y, Li K, Zhao Y, Tang W, Huang J, Wang W, Xie J. Anti-*Foc* RT4 activity of a newly isolated *Streptomyces* sp. 5–10 from a medicinal plant (*Curculigo capitulata*). Front Microbiol. 2021;11:610698.
4. Cao M, Cheng Q, Cai B, Chen Y, Wei Y, Qi D, Li Y, Yan L, Li X, Long W, Liu Q, Xie J, Wang W. Antifungal mechanism of metabolites from newly isolated *Streptomyces* sp. Y1-14 against banana *Fusarium* wilt using metabolomics. J Fungi (Basel). 2022;8(12):1291.
5. Tripathi L, Ntui VO, Tripathi JN. CRISPR/Cas9-based genome editing of banana for disease resistance. Curr Opin Plant Biol. 2020;56:118–26.
6. Bubici G, Kaushal M, Prigigallo MI, Gómez-Lama Cabanás C, Mercado-Blanco J. Biological control agents against *Fusarium* wilt of banana. Front Microbiol. 2019;10:616.
7. Guzmán-Guzmán P, Kumar A, de los Santos-Villalobos S, Parra-Cota FI, Orozco-Mosqueda MC, Fadiji AE, Hyder S, Babalola OO, Santoyo G. *Trichoderma* species: our best fungal allies in the biocontrol of plant diseases-A review. Plants (Basel). 2023;12(3):432.
8. Woo SL, Hermosa R, Lorito M, Monte E. *Trichoderma*: a multipurpose, plant-beneficial microorganism for eco-sustainable agriculture. Nat Rev Microbiol. 2023;21(5):312–26.
9. Joo JH, Hussein KA. Biological control and plant growth promotion properties of volatile organic compound-producing antagonistic *Trichoderma spp.* Front Plant Sci. 2022;13:897668.
10. Rajani P, Rajasekaran C, Vasanthakumari MM, Olsson SB, Ravikanth G, Uma Shaanker R. Inhibition of plant pathogenic fungi by endophytic *Trichoderma spp.* through mycoparasitism and volatile organic compounds. Microbiol Res. 2021;242:126595.
11. Tomah AA, Abd Alamer IS, Li B, Zhang J-Z. A new species of *Trichoderma* and Gliotoxin role: a new observation in enhancing biocontrol potential of *T. virens* against *Phytophthora capsici* on Chili pepper. Biol Control. 2020;145:104261.
12. Díaz-Gutiérrez C, Arroyave C, Llugany M, Poschenrieder C, Martos S, Peláez C. *Trichoderma Asperellum* as a preventive and curative agent to control *Fusarium* wilt in *Stevia rebaudiana*. Biol Control. 2021;155.
13. Andrzejak R, Janowska B. *Trichoderma spp.* improves flowering, quality, and nutritional status of ornamental plants. Int J Mol Sci. 2022;23(24):15662.

14. Samuelian S. Potential of *Trichoderma Harzianum* for control of banana leaf fungal pathogens when applied with a food source and an organic adjuvant. 3 Biotech. 2016;6(1):8.
15. Savani AK, Bhattacharyya A, Boro RC, Dinesh K, Jc N. Exemplifying endophytes of banana (*Musa Paradisiaca*) for their potential role in growth stimulation and management of *Fusarium oxysporum* f. sp *cubense* causing Panama wilt. Folia Microbiol (Praha). 2021;66:317–30.
16. Kramer J, Ozkaya O, Kummerli R. Bacterial siderophores in community and host interactions. Nat Rev Microbiol. 2020;18:152–63.
17. Wang W, Qiu Z, Tan H, Cao L. Siderophore production by actinobacteria. Biometals. 2014;27:623–31.
18. Vinale F, Nigro M, Sivasithamparam K, Flematti G, Ghisalberti EL, Ruocco M, Varlese R, Marra R, Lanzuise S, Eid A, Woo SL, Lorito M. Harzianic acid: a novel siderophore from *Trichoderma Harzianum*. FEMS Microbiol Lett. 2013;347(2):123–9.
19. Schalk IJ, Hannauer M, Braud A. New roles for bacterial siderophores in metal transport and tolerance. Environ Microbiol. 2011;13(11):2844–54.
20. Sharma A, Johri BN. Growth promoting influence of siderophore-producingpseudomonas strains GRP3A and PRS9 in maize (*Zea mays* L.) under iron limiting conditions. Microbiol Res. 2003;158(3):243–8.
21. Sulochana MB, Jayachandra SY, Kumar SA, Parameshwar AB, Reddy KM, Dayanand A. Siderophore as a potential plant growth-promoting agent produced by *Pseudomonas aeruginosa* JAS-25. Appl Biochem Biotechnol. 2014;174(1):297–308.
22. Di Francesco A, Baraldi E. How siderophore production can influence the biocontrol activity of *Aureobasidium pullulans* against *Monilinia laxa* on peaches. Biol Control. 2021;152.
23. Zhao L, Wang Y, Kong S. Effects of *Trichoderma Asperellum* and its siderophores on endogenous auxin in *Arabidopsis thaliana* under iron-deficiency stress. Int Microbiol. 2020;23:501–9.
24. Manganiello G, Sacco A, Ercolano MR, Vinale F, Lanzuise S, Pascale A, Napolitano M, Lombardi N, Lorito M, Woo SL. Modulation of tomato response to *Rhizoctonia solani* by *Trichoderma Harzianum* and its secondary metabolite harzianic acid. Front Microbiol. 2018;9:1966.
25. Long W, Chen Y, Wei Y, Feng J, Zhou D, Cai B, Qi D, Zhang M, Zhao Y, Li K, et al. A newly isolated *Trichoderma Parareesei* N4-3 exhibiting a biocontrol potential for banana *Fusarium* wilt by hyperparasitism. Front Plant Sci. 2023;14:1289959.
26. Wang YJ, Huang W, Ali SW, Li YQ, Yu FB, Deng HH. Isolation, identification, and characterization of an efficient siderophore producing bacterium from heavy metal contaminated soil. Curr Microbiol. 2022;79(8):227.
27. Wang N, Wang T, Chen Y, et al. Microbiome convergence enables siderophore-secreting-rhizobacteria to improve iron nutrition and yield of peanut intercropped with maize. Nat Commun. 2024;15(1):839.
28. Wei Y, Zhao Y, Zhou D, Qi D, Li K, Tang W, Chen Y, Jing T, Zang X, Xie J, Wang W. A newly isolated *Streptomyces* sp. YYS-7 with a broad-spectrum antifungal activity improves the banana plant resistance to *Fusarium oxysporum* f. sp. *cubense* tropical race 4. Front Microbiol. 2020;11:1712.
29. Koren S, Walenz BP, Berlin K, Miller JR, Bergman NH, Phillippy AM. Canu: scalable and accurate long-read assembly via adaptive *k*-mer weighting and repeat separation. Genome Res. 2017;27:722–36.
30. Zeng J, Xu T, Cao L, Tong C, Zhang X, Luo D,Han S, Pang P, Fu W, Yan J, Liu X, Zhu Y. The role of iron competition in the antagonistic action of the rice endophyte *Streptomyces sporocinereus* OsiSh-2 against the pathogen *Magnaporthe oryzae*. Microb Ecol. 2018;76(4):1021–9.
31. Shenker M, Oliver I, Helmann M, Hadar Y, Chen Y. Utilization by tomatoes of iron mediated by a siderophore produced by *Rhizopus Arrhizus*. J Plant Nutr. 2008;15:2173–82.
32. Sheng M, Jia H, Zhang G, Zeng L, Zhang T, Long Y, Lan J, Hu Z, Zeng Z, Wang B, Liu H. Siderophore production by rhizosphere biological control bacteria *brevibacillus brevis* GZDF3 of *Pinellia ternata* and its antifungal effects on *Candida albicans*. J Microbiol Biotechnol. 2020;30:689–99.
33. Wang Y, Zhang G, Huang Y, Guo M, Song J, Zhang T, Long Y, Wang B, Liu H. A potential biofertilizer-siderophilic bacteria isolated from the rhizosphere of Paris polyphylla var. Yunnanensis. Front Microbiol. 2022;13:870413.
34. Gu S, Wei Z, Shao Z, Friman VP, Cao K, Yang T, Kramer J, Wang X, Li M, Mei X, Xu Y, Shen Q, Kümmerli R, Jousset A. Competition for iron drives phytopathogen control by natural rhizosphere microbiomes. Nat Microbiol. 2020;5(8):1002–10.
35. Zhang L, Liu Z, Wang Y, Zhang J, Wan S, Huang Y, Yun T, Xie J, Wang W. Biocontrol potential of endophytic *Streptomyces malaysiensis* 8ZJF-21 from medicinal plant against banana *Fusarium* wilt caused by *Fusarium oxysporum* f. sp. Cubense Trop Race 4 Front Plant Sci. 2022;13:874819.
36. Zhang L, Zhang H, Huang Y, Peng J, Xie J, Wang W. Isolation and evaluation of rhizosphere actinomycetes with potential application for biocontrolling *Fusarium* wilt of banana caused by *Fusarium oxysporum* f. sp. *cubense* tropical race 4. Front Microbiol. 2021;12:763038.
37. Peraza-Jiménez K, De la Rosa-García S, Huijara-Vasconselos JJ, Reyes-Estebanez M, Gómez-Cornelio S. Enzymatic bioprospecting of fungi isolated from a tropical rainforest in Mexico. J Fungi (Basel). 2021;8(1):22.
38. Damodaran T, Rajan S, Muthukumar M, Ram G, Yadav K, Kumar S, Ahmad I, Kumari N, Mishra VK, Jha SK. Biological management of banana Fusarium wilt caused by *Fusarium oxysporum* f. sp. *cubense* tropical race 4 using antagonistic fungal isolate CSR-T-3 (*Trichoderma reesei*). Front Microbiol. 2020;11:595845.
39. Swain H, Adak T, Mukherjee AK, Mukherjee PK, Bhattacharyya P, Behera S, Bagchi TB, Patro R, Shasmita, Khandual A, Bag MK, Dangar TK, Lenka S, Jena M. Novel Trichoderma strains isolated from tree barks as potential biocontrol agents and biofertilizers for direct seeded rice. Microbiol Res. 2018;214:83–90.
40. Dou K, Lu Z, Wu Q, Ni M, Yu C, Wang M, Li Y, Wang X, Xie H, Chen J, Zhang C. MIST: a multilocus identification system for *Trichoderma*. Appl Environ Microbiol. 2020;86(18):e01532–20.
41. Chowdappa S, Jagannath S, Konappa N, Udayashankar AC, Jogaiah S. Detection and characterization of antibacterial siderophores secreted by endophytic fungi from *Cymbidium aloifolium*. Biomolecules. 2020;10(10):1412.
42. Boiteau RM, Markillie LM, Hoyt DW, Hu D, Chu RK, Mitchell HD, Pasa-Tolic L, Jansson JK, Jansson C, Bulgarelli D. Metabolic interactions between *Brachypodium* and *Pseudomonas fluorescens* under controlled iron-limited conditions. mSystems. 2021;6(1):e00580–20.
43. Holzberg M, Artis WM. Hydroxamate siderophore production by opportunistic and systemic fungal pathogens. Infect Immun. 1983;40(3):1134–9.
44. Clarke TE, Braun V, Winkelmann G, Tari LW, Vogel HJ. X-ray crystallographic structures of the *Escherichia coli* periplasmic protein FhuD bound to hydroxamate-type siderophores and the antibiotic albomycin. J Biol Chem. 2002;277:13966–72.
45. Pandey SS, Patnana PK, Rai R, Chatterjee S. Xanthoferrin, the alpha-hydroxycarboxylate-type siderophore of *Xanthomonas campestris* Pv. *Campestris*, is required for optimum virulence and growth inside cabbage. Mol Plant Pathol. 2017;18:949–62.
46. López AC, Alvarenga AE, Zapata PD, Luna MF, Villalba LL. *Trichoderma* spp. from Misiones, Argentina: effective fungi to promote plant growth of the regional *cropllex paraguariensis* St. Hil. Mycology. 2019;10:210–21.
47. Druzhinina IS, Seidl-Seiboth V, Herrera-Estrella A, Horwitz BA, Kenerley CM, Monte E, Mukherjee PK, Zeilinger S, Grigoriev IV, Kubicek CP. *Trichoderma*: the genomics of opportunistic success. Nat Rev Microbiol. 2011;9:749–59.
48. Lorito M, Woo SL, Harman GE, Monte E. Translational research on *Trichoderma*: from 'omics to the field. Annu Rev Phytopathol. 2010;48:395–417.
49. Liu B, Ji S, Zhang H, Wang Y, Liu Z. Isolation of *Trichoderma* in the rhizosphere soil of *Syringa oblata* from Harbin and their biocontrol and growth promotion function. Microbiol Res. 2020;235:126445.
50. Guo K, Sui Y, Li Z, Huang Y, Zhang H, Wang W. Colonization of *Trichoderma viride* Tv-1511 in peppermint (*Mentha* x *piperita* L.) roots promotes essential oil production by triggering ROS-mediated MAPK activation. Plant Physiol Biochem. 2020;151:705–18.
51. Garstecka Z, Antoszewski M, Mierek-Adamska A, et al. *Trichoderma viride* colonizes the roots of *brassica napus* L., alters the expression of stress-responsive genes, and increases the yield of canola under field conditions during drought. Int J Mol Sci. 2023;24(20):15349.

Publisher's note